Talanta 115 (2013) 506–511

Contents lists available at SciVerse ScienceDirect

Talanta

journal homepage: www.elsevier.com/locate/talanta

Double-functionalized gold nanoparticles with split aptamer for the detection of adenosine triphosphate

Sheng Cheng [a,b], Bin Zheng [a,b], Mozhen Wang [b], Michael Hon-Wah Lam [a,*], Xuewu Ge [b,**]

[a] Department of Biology and Chemistry, City University of Hong Kong and USTC-CityU Joint Advanced Research Center, Suzhou, PR China
[b] CAS Key Laboratory of Soft Matter Chemistry, Department of Polymer Science and Engineering, University of Science and Technology of China and USTC-CityU Joint Advanced Research Center, Suzhou, PR China

ARTICLE INFO

Article history:
Received 15 May 2013
Accepted 28 May 2013
Available online 2 June 2013

Keywords:
Gold nanoparticles
Double-functionalization
Split aptamer
Colorimetric sensing
Adenosine triphosphate

ABSTRACT

A newly designed functionalization type for gold nanoparticles (AuNP) with split aptamer has been developed for the detection of adenosine triphosphate (ATP). The ATP aptamer was split into two parts with their 5′ prime or 3′ prime modified with thiol. Both the 5′ SH and 3′ SH modified strands for each split aptamer fragment were functionalized onto the same AuNP to construct double-functionalized AuNP–DNA conjugates. Thus, the split aptamer can be reassembled into intact folded structure in the presence of ATP molecule with two potential assembly types, which induces the assembly of AuNP–DNA conjugates. In this double-functionalized system, the traditional assembly type might facilitate another assembly type, which was found to give much higher LSPR change in the presence of ATP than the traditional assembly type, and improve the sensitivity for ATP detection. Time courses of the assemble processes with different assembly types, Mg^{2+} concentrations, and aptamer fragments densities on AuNP were followed using the absorption ratio at 650 nm and 520 nm. ATP response with this newly designed system was investigated using absorption spectra and dynamic light scattering method.

1. Introduction

Gold nanoparticles (AuNPs) are excellent colorimetric probes because of their unique localized surface plasmon resonance (LSPR) optical properties [1–3] and high extinction coefficient (3–5 orders of magnitude higher than that of organic chromophores) [4]. Since the development of attaching thiolated DNA to AuNPs in the year 1996 [5,6], the DNA-directed assembly of nanoparticles has become a hot method and expanded its applications in various fields, including nanoparticles preparation and sorting, biosensing and biomedicine [7–10]. One of the emerging fields is aptamer-based biosensing. Aptamers are single-stranded oligonucleotides with tailor-made sequences—as versatile receptors for high-affinity analyte binding [11]. Their sequence of nucleotides that enable them to specifically bind to their targeted analytes, with dissociation constants in the range of micromolar to picomolar, are generally determined through the SELEX (systematic evolution of ligands by exponential enrichment) process [12,13]. The high affinity, chemical stability, small size and convenience in synthesis, storage and modification make aptamer an excellent receptor to design biosensors [14].

Up to now, many elegant ways have been proposed to transduce aptamer-target binding event to visible signals of AuNPs [15,16]. One effective way is to covalently conjugate AuNP with DNA to achieve the purpose of target directed assembly or disassembly of AuNPs, which leads to red-purple color switch of AuNP solution. Lu's group reported a fast colorimetric sensing method for small molecules [17,18]. In their system, DNA–AuNP conjugates were assembled by a linker strand which contains aptamer sequence. The linker strand folded up in the presence of target molecules and disassembled the aggregates. Fan's group improved this approach by attaching split aptamer strands onto different AuNPs [19]. In this system, the presence of target molecules combined with split aptamers and formed intact folded structures. Thus, the target molecules acted as a molecular linker which directly assembled AuNPs and induced color change. The aptamer split is an important technique in novel biosening design, such as sandwich-format biosensor [20]. The specific binding affinity between aptamer and target makes it possible to reassemble into intact aptamer structure when the split aptamers fragments encounter their targets. This technique facilitates the strategy design toward biosensing systems based on colorimetry [19,21–24], fluorescence [25,26], electrochemical technology [20,27–30], surface plasmon resonance [31], and dynamic light scattering [32].

* Correspondence to: Department of Biology & Chemistry, City University of Hong Kong, Tat Chee Ave., Kowloon, Hong Kong SAR, PR China. Tel.: +852 3442 7329.
** Correspondence to: CAS Key Laboratory of Soft Matter Chemistry, Department of Polymer Science and Engineering, University of Science and Technology of China, PR China. Tel.: +86 551 6360 7410.
E-mail addresses: bhmhwlam@cityu.edu.hk (M.-W. Lam), xwge@ustc.edu.cn (X. Ge).

0039-9140/$ - see front matter Crown Copyright © 2013 Published by Elsevier B.V. All rights reserved.
http://dx.doi.org/10.1016/j.talanta.2013.05.065

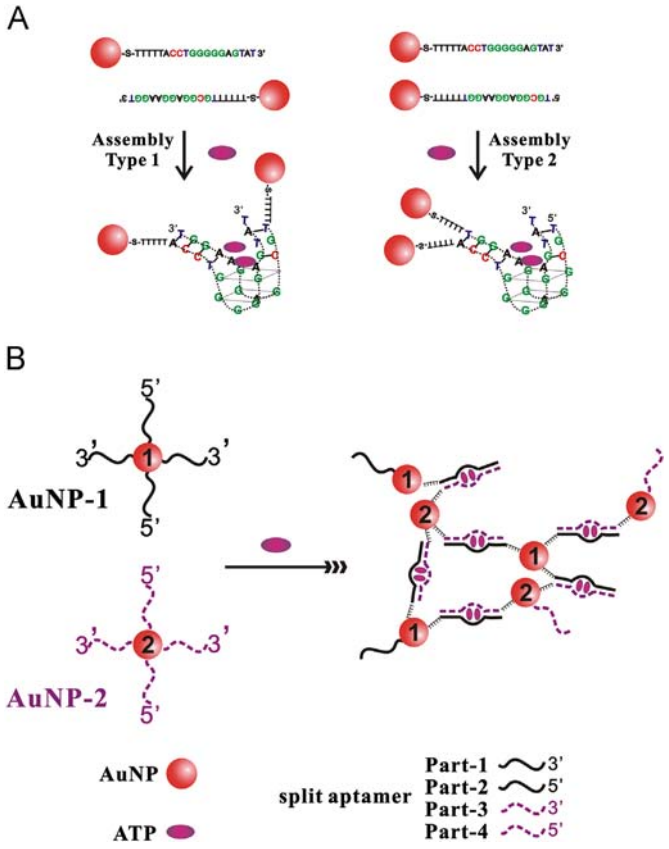

Fig. 1. (A) Two assembly types of AuNPs functionalized with different split ATP aptamer. (B) Sensing scheme of the double-functionalized AuNP-split aptamer system for ATP.

In the strategies of target directed assembly or disassembly of AuNPs, the traditional design of DNA–AuNP conjugates is to locate AuNPs at the two ends of the folded structures [17,19,32,33], which is similar to Assembly Type 1 in Fig. 1A. Obviously, the strategy of Assembly Type 2 (Fig. 1A) may produce higher LSPR change because the distance between AuNPs is much closer after binding with target. However, in this work, it was found out that the assembly rate of Type 2 was too slow which was not appropriate for sensing. Here, we proposed a new functionalization strategy by combining Assembly Type 1 and Type 2. In this work, we designed a double-functionalized AuNP–DNA system for the detection of adenosine triphosphate (ATP). ATP plays crucial roles in the regulation of cellular metabolism and has been widely used as an index in biomass determinations in clinical microbiological assays, food quality control and environmental analyses [34,35]. Thus, the detection of ATP is of great importance. As shown in Fig. 1B, each split aptamer fragment is modified onto the same AuNPs at its 5′ prime or 3′ prime. The results show that this double-functionalized AuNP–DNA system can produce higher LSPR change than the traditional one and high response rate simultaneously.

2. Experimental

2.1. Materials and apparatus

All oligonucleotides (HPLC grade) and fetal calf serum were purchased from Sangon Biotechnology Inc. (Shanghai, China). The base sequences are listed in Table 1. DNA stock solutions were prepared by dissolving oligonucleotides in water. Their concentrations

Table 1
List of sequences.

Designation of strand	Sequence
Part-1	5′-HS-TTTTTACCTGGGGGAGTAT-3′
Part-2	5′-ACCTGGGGGAGTATTTTTT-SH-3′
Part-3	5′-HS-TTTTTTGCGGAGGAAGGT-3′
Part-4	5′-TGCGGAGGAAGGTTTTTT-SH-3′
Poly-T5	5′-SH-TTTTT-3′
Control sequence	5′-SH-TTTTTCATTTCCCCCCATC

were determined by measuring their UV absorbance at 260 nm. The extinction coefficient (ε) for each nucleotide was: ε(dA)= 15400 M^{-1} cm^{-1}, ε(dG)=11500 M^{-1} cm^{-1}, ε(dC)=7400 M^{-1} cm^{-1}, and ε(dT)=8700 M^{-1} cm^{-1}. Adenosine 5′-triphosphate disodium salt (ATP), uridine 5′-triphosphate trisodium salt (UTP), cytidine 5′-triphosphate disodium salt (CTP) and guanosine 5′-triphosphate sodium salt (GTP) were purchased from Sigma. All the other reagents (analytical reagent) were purchased from Sinopharm Chemical Reagent Co., Ltd. (Shanghai, China), and were used as received. Milli-Q water (18.2 MΩ cm) (Millpore Co., USA) was used throughout the study.

Time course files of assembly processes and UV–vis absorption spectra were recorded using a Shimadzu UV-1800 UV–vis spectrophotometer equipped with a circular water bath to keep temperature constant. Quick measurements of DNA concentration were conducted with a Thermo Scientific NanoDrop 1000 Spectrophotometer. The hydrodynamic diameters of AuNPs were measured using a dynamic light scattering particle size analyzer (Malvern Zetasizer Nano ZS).

2.2. Synthesis of gold nanoparticles (AuNPs)

Gold nanoparticles of ca. 13 nm in diameter were synthesized using the citrate reduction method [36,37]. Briefly, trisodium citrate solution (10 mL, 38 mM) was added to a boiling chloroauric acid solution (100 mL, 1 mM) with vigorous stirring. The color of the mixed solution changed from pale yellow to gray, black, blue, purple, and finally to red within two minutes. The solution was stirred for an additional 15 min and gradually cooled to room temperature. The AuNP solution was stored at 4 °C before use after being filtered through a 0.22 μm membrane. To measure the concentration of AuNPs, an appropriate volume of the AuNPs stock solution was diluted for 5 times with ultra-pure water and the absorbance at 520 nm was measured by UV–vis spectrophotometer. The nanoparticle concentration was estimated with the reported molar extinction coefficients at 520 nm ($\varepsilon = 2.7 \times 10^8$ M^{-1} cm^{-1}) [38].

2.3. Preparation of AuNPs–DNA conjugates

AuNPs were double-functionalized with split aptamer fragments *via* the gold–sulfur chemical bonds. AuNP-1 was prepared through conjugating AuNPs with Part-1, Part-2 and Poly-T5 according to literature with minor modifications [37]. Briefly, 20 μL of DNA solution containing Part-1, Part-2 and Poly-T5 (total concentration was 100 μM) were mixed with 0.6 μL of Tris-(2-carboxyethyl) phosphine hydrochloride (TCEP) (30 mM) and 2 μL of Acetate buffer (sodium acetate and acetic acid) (500 mM, pH 5.2). The above mixture was incubated at room temperature for 1 h, and then 400 μL of AuNPs solution (11 nM) was added. After 16 h incubation, 5 μL of Tris–acetate buffer (500 mM, pH 8.2) and 48 μL of NaCl solution (1 M) were introduced, and another 24 h incubation procedure was needed to complete the functionalization. The mixture was centrifuged at 15,000 rpm for 15 min, and the supernatant was removed. The deposition was rinsed with Tris–EDTA buffer (10 mM, pH 8.0) (TE buffer) for three times through centrifugation. The final resultant was resuspended in 800 μL

of TE buffer and stored at 4 °C for further use. Likewise, AuNP-2 was prepared through conjugating AuNPs with Part-3, Part-4 and Poly-T5 with the same protocol. In each functionalization experiment, the amount ratio of 5′ SH to 3′ SH split aptamer fragment was 1:1 and that of total DNA to AuNPs was 450:1.

2.4. ATP response

The time courses of the assembly process were recorded on Shimadzu UV-1800 UV–vis spectrophotometer with the kinetics model. 100 μL of AuNP-1 and 100 μL of AuNP-2 were mixed with 20 μL of ATP solution (11 mM) containing 220 mM $MgCl_2$. The reactant solution was rapidly moved into quartz cuvette, and the absorption at 520 nm and 650 nm was recorded every 12 s.

In ATP detection assays, ATP solutions of various concentrations (20 μL) containing 220 mM $MgCl_2$ were incubated with 100 μL of AuNP-1 and 100 μL of AuNP-2 solutions. The resultant mixtures were incubated at 20 °C for 1.5 h and their absorption spectra were recorded from 400 to 800 nm. To determine the aggregation of AuNPs, the resultant mixtures were analyzed on a dynamic light scattering (DLS) particle size analyzer (Malvern Zetasizer Nano ZS) under the following conditions: temperature 25 °C, detector angle 173°, incident laser wavelength 633 nm, laser power 4.0 mW. To determine the selectivity of the biosensing, the assays were repeated with water (blank), and solutions of CTP, GTP and UTP. Concentration of all the analytes was 1 mM. To assess the sequence specificity, the control sequence was functionalized onto AuNPs with the same processes and experimental conditions as the preparation of AuNP-1, and its response to 1 mM ATP was performed.

The ATP detection assay in real samples was conducted according to the method reported by Tang with minor modifications [39]. Briefly, 3 samples containing 100 μM, 200 μM and 400 μM ATP, were prepared by spiking ATP standards into blank fetal calf serum. The mixed solutions were used to repeat the above ATP detection procedures.

3. Results and discussion

3.1. Design and working principle of the double-functionalized AuNP–DNA sensing system

The DNA aptamer for ATP was developed in the year 1995 [40]. This aptamer contains two highly conserved guanine-rich regions, two invariant adenine residues and two regions of predominant Watson–Crick co variation. The 27-mer DNA aptamer can bind ATP with the dissociation constant of 6 ± 3 μM. Up to now, many research have proved that the split ATP aptamer can reassemble into the intact G-quadruple structure with ATP [28,30–32]. Therefore, the ATP aptamer was split according to the literature [19] to carry out further study in our work.

As shown in Fig. 1, two assembly types can be designed according to the location of AuNPs on DNA strands. Assembly Type 1 is the traditional design in target directed assembly of AuNPs. The distance-dependent optical property of AuNPs indicates that the system of Assembly Type 2 may produce higher LSPR change because the distance between AuNPs is much closer after binding with ATP. We studied the time course of the assembly process of Type 1 and Type 2 (Fig. 2, Line 1 and Line 2). Here, the common used absorption ratio at 650 nm and 520 nm of AuNPs solution (A_{650}/A_{520}) was used to reflect the aggregation of AuNPs. It is clearly seen that the traditional Type 1 gave a fast assembly rate in the presence of 1 mM ATP and reached plateau in 30 min, while the Type 2 gave a very low assembly rate and could not reach plateau even in 90 min. The low assembly rate of Type 2 may be caused by the large steric hindrance given by AuNPs which hinder the formation of G-quadruple structure from two split aptamer fragments and ATP or make the formed structure unstable. Therefore, we designed a double-functionalized AuNP–DNA sensing system which combined Assembly Type 1 and Type 2 (Fig. 1B). As shown in Fig. 1B and Table 1, each split aptamer fragments has 5′ SH modified sequence and 3′ SH modified sequence, such as Part-1 and Part-2. They were functionalized onto the same AuNP. The AuNPs which conjugate with Part-1 and Part-2 are designated as AuNP-1 and that with Part-3 and Part-4 are designated as AuNP-2. The time course of the assembly process of the double-functionalized system is shown in Fig. 2 (Line 4). The assembly rate of our newly designed system was greatly improved, and what is more, the LSPR change in 90 min was much larger than the traditional one (Type 1). In order to explore the possible explanations to this phenomenon, another assay was conducted. The DNA sequences Part-1, Part-2, Part-3 and Part-4 were attached to four kinds of AuNPs respectively. After treated with the same processes and experimental conditions as the preparation of AuNP-1 and AuNP-2, 50 μL of each single-functionalized AuNP–DNA conjugate were mixed with 20 μL of ATP solution (11 mM) containing 220 mM $MgCl_2$. The time course data is shown in Fig. 2 (Line 3). The assembly process was very similar to that of Type 1. Thus, we conclude that only the AuNPs double-functionalized with 5′ SH and 3′ SH split aptamer fragments can produce higher LSPR change. We infer that both Assembly Type 1 and Type 2 occurred in the double-functionalized AuNP–DNA system, and the occurrence of Type 2 greatly increased the LSPR change. Because the 5′ SH and 3′ SH split aptamer fragments were attached on the same AuNP, the occurrence of Assembly Type 1, such as the assembly from Part-1, Part-3 and ATP, provided opportunity to the assembly from Part-1 and Part-4 on another AuNP in this aggregates. Thus, the occurrence of Assembly Type 1 facilitates the occurrence of Assembly Type 2, which makes Type 2 donate a considerable fraction in LSPR change. However, this assistance from Type 1 is hard to occur in the system of the mixture of four single-functionalized AuNP–DNA, because these DNA sequences (Part-1, Part-2, Part-3 and Part-4) were attached on different AuNPs, and the assembly prone to occur between conjugates with fast rate and low steric hindrance. Therefore, the double-functionalized AuNP–DNA system can provide higher LSPR change and may be promising in the enhancement of sensing sensitivity.

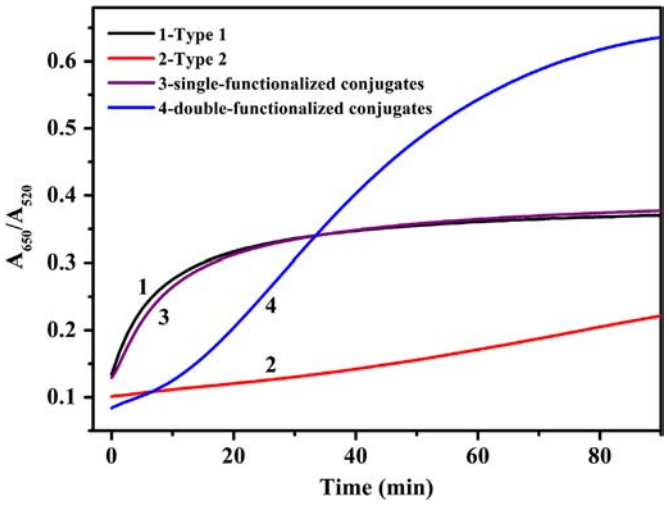

Fig. 2. Time course of the assembly process of different functionalization types in the presence of 1 mM ATP. The molar ratio of split aptamer to Poly-T5 spacer was 1:1 and the final concentration of Mg^{2+} was 20 mM.

The assembly behavior of the designed double-functionalized DNA–AuNPs system (as shown in Fig. 2) is different from others.

There seems to be an "induction" time at the beginning 15 min. From Fig. 2, Line 4, it can be seen that the aggregation rate is slower than Assembly Type 1 (Line 1) but still faster than Assembly Type 2 (Line 2) at the beginning 15 min. We infer that this is mainly caused by the occurrence of Assembly Type 1. Because the split aptamer fragments were prepared for Assembly Type 1 and Type 2 in the double-functionalized system, the amount of the functional fragments for Assembly Type 1 is sparser than the normal one, which produced a slower rate. The Assembly Type 2 cannot donate a considerable fraction because of its high steric hindrance at the beginning. However, with the aggregation of the double-functionalized AuNPs, more sites which are beneficial for the occurrence of Assembly Type 2 emerge on the aggregates. The occurrence of Assembly Type 2 greatly increases the LSPR response and the increasing aggregation rate in Line 4 after 15 min is observed. Therefore, from the assembly behavior of the newly designed system, we infer that the Assembly Type 1 dominates the aggregation at the beginning and then the Assembly Type 2 participates in the assembly of AuNPs.

3.2. Effect of Mg^{2+} concentrations and aptamer fragments densities

The presence of Mg^{2+} is required for aptamer folding in the presence of ATP, but not affects the conformation of aptamer in the absence of ATP [41]. We studied the effect of Mg^{2+} concentrations on the assembly of AuNP–DNA conjugates in the presence and absence of ATP. In Fig. 3, the assembly rate increased with the increase of Mg^{2+} concentration. However, the assembly also occurred in the absence of ATP. This is caused by the Mg^{2+} induced aggregation of AuNPs, even they have been functionalized with DNAs [41]. Thus, an appropriate Mg^{2+} concentration should be determined to optimize the sensing system. By comparing the value differences of A_{650}/A_{520} in the presence and absence of ATP, we conclude that of 20 mM Mg^{2+} (final concentration) can give the largest LSPR change.

The DNA strand Poly-T5 was used to adjust the function DNA density and improve the stability of AuNPs in our work. Here, different aptamer fragment to Poly-T5 ratios (Apt-T5 ratios) were investigated. Fig. 4 displays the time courses of assembly process in the systems with different Apt-T5 ratios. The assembly process became faster when the Apt-T5 ratios varied from 4:1 to 1:1, while it became slower when the Apt-T5 ratios varied from 1:1 to 1:4. The assembly rate reached a maximum when the ratio was given to 1:1. This result can be interpreted by the steric hindrance of DNA strands and assembly stability. When the Apt-T5 ratio was high, the aptamer fragment was too dense on the surface of AuNP, and the adjacent DNA strands might hinder the assembly process. When the Apt-T5 ratio was low, the aptamer fragment was sparse, which made the assembled aggregate easily be dispersed due to the electrostatic repulsion between AuNP–DNA conjugates.

3.3. Sensitivity and selectivity

We here designed a double-functionalized AuNP–DNA sensing system which relied on the target directed assembly of AuNP–DNA conjugates. After the optimization of Mg^{2+} concentrations and aptamer fragments densities on AuNPs, we herein conducted the assays to estimate the sensitivity of this sensing system for ATP. Fig. 5A shows the UV–vis spectra of AuNP–DNA solutions in the presence of various concentrations of ATP. The addition of ATP shifted the SPR absorption to the longer wave-length. With the increase of ATP concentrations, the absorption at 520 nm decreased and that around 650 nm increased. The absorption ratio at 650 nm and 520 nm of AuNPs solution (A_{650}/A_{520}) vs. ATP concentrations was plotted in Fig. 5B. The limit of detection which was determined to be 24 μM ($S/N \geq 3$) is more sensitive than traditional assembly sensing system [19]. A relative standard deviation (RSD) was calculated to be 2.3% by 10 repetitive measurements of 400 μM ATP, demonstrating a high accuracy and reproducibility of the assay. From these results, we can see that our designed double-functionalized AuNP–DNA sensing system is highly sensitive to ATP. To demonstrate that the spectra variation was induced by AuNP aggregation, we conducted DLS measurements of the AuNP–DNA conjugates assembled by ATP. As shown in Fig. 6, the hydrodynamic diameters of AuNPs increased gradually with the ATP concentration varying from 0 to 5 mM. To assess the selectivity of the biosensing system, control experiments were performed on ATP analogs—UTP, CTP and GTP. Fig. 7 summarizes the outcomes. Only ATP can induce high LSRP change. A control sequence which has the same length with split aptamer was functionalized on AuNPs to explore whether the assembly had sequence specificity. The result in Fig. 7 demonstrates that only split ATP aptamer–AuNP conjugates can result the assembly with ATP molecules. The good analyte selectivity is attributable to the high specificity of the aptamer for ATP-binding. We further evaluated the possibility of this double-functionalized DNA–AuNPs system in real sample detection. The ATP standards and their detection results with RSD% by our designed method have been

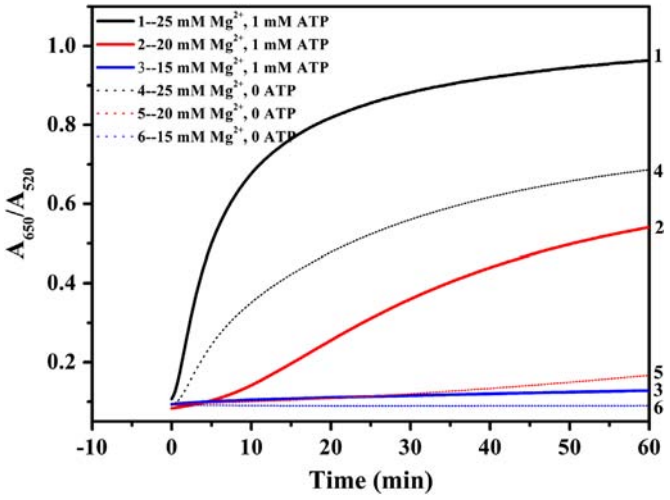

Fig. 3. Time course of the assembly process of the double-functionalized AuNP–DNA conjugates in the presence of different concentrations of Mg^{2+}. The molar ratio of split aptamer to Poly-T5 spacer was 1:1.

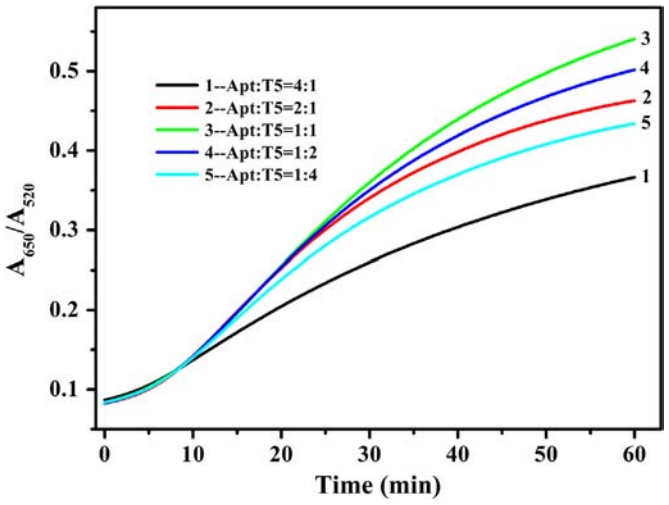

Fig. 4. Time course of the assembly process of the double-functionalized AuNP–DNA conjugates with different molar ratios of split aptamer to Poly-T5. The concentration of Mg^{2+} was 20 mM.

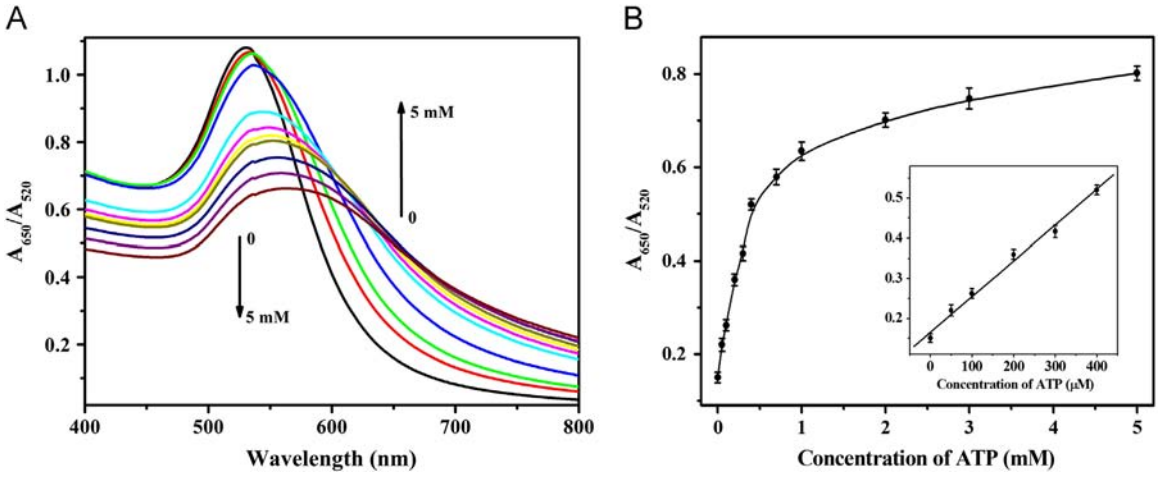

Fig. 5. (A) UV–vis spectra of the double-functionalized AuNP–DNA sensing system in the presence of different concentrations of ATP. (B) Absorption ratio (A_{650}/A_{520}) of AuNPs solution vs. ATP concentrations. Inset: The enlarged section from 0–400 μM. The molar ratio of split aptamer to Poly-T5 spacer was 1:1 and the final concentration of Mg^{2+} was 20 mM.

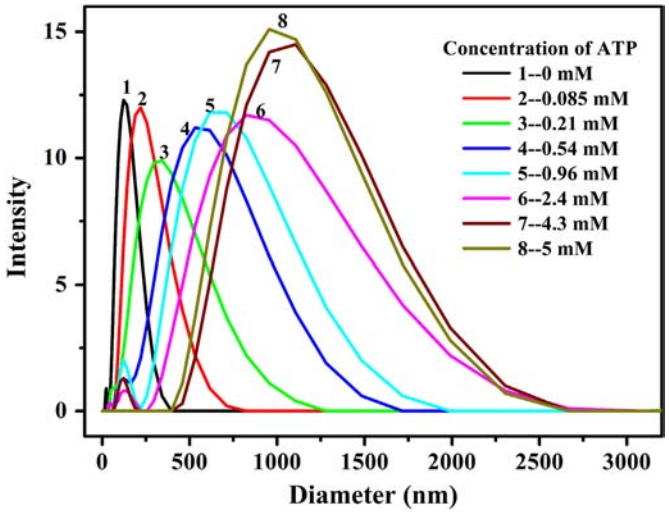

Fig. 6. DLS analysis data of the double-functionalized AuNP–DNA conjugates in the presence of different concentrations of ATP. The molar ratio of split aptamer to Poly-T5 spacer was 1:1 and the final concentration of Mg^{2+} was 20 mM.

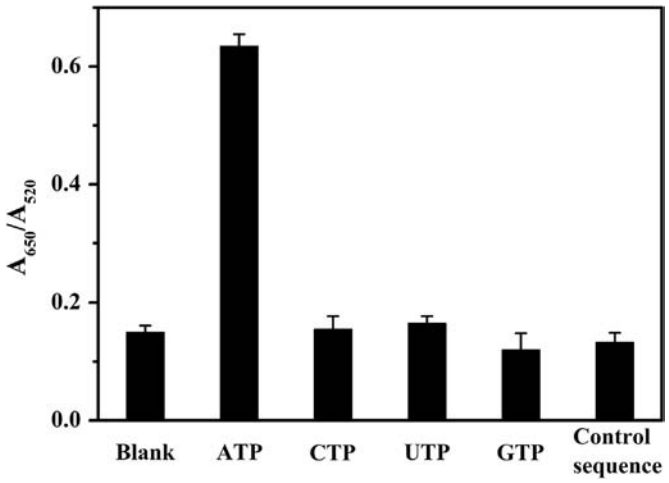

Fig. 7. Absorption ratios (A_{650}/A_{520}) of the double-functionalized AuNP–DNA system toward ATP, UTP, CTP, GTP and blank samples, and that of the control sequence functionalized AuNP system toward ATP. The molar ratio of split aptamer to Poly-T5 spacer was 1:1 and the final concentration of Mg^{2+} was 20 mM.

Table 2
Analysis of ATP in fetal calf serum.

Sample	ATP standards (μM)	ATP concentration using this method (μM)	RSD (%, $n=5$)
1	100	107.3	4.7
2	200	205.0	2.7
3	400	392.7	3.0

listed in Table 2. It can be seen that this double-functionalized DNA–AuNPs system has provided accuracy detection results with good repeatability, indicating its feasibility in real sample detection.

4. Conclusion

In summary, a double-functionalized AuNP-split aptamer system has been developed for the detection of ATP. The ATP directed assembly process of this double-functionalized AuNP–DNA system might adopt two assembly types and was found to give higher LSPR change than the traditional assembly type. In this double-functionalized system, the traditional assembly type might facilitate another assembly type, which provided much higher LSPR change in the presence of ATP than the traditional assembly type, and improved the sensitivity for ATP detection. After the optimization of Mg^{2+} concentration and aptamer fragments densities on AuNPs, the limit of detection of the newly designed system was determined to be 24 μM, which was more sensitive than the system constructed from traditional assemble type. Furthermore, such strategy utilizing double-functionalized AuNP–DNA system can also be applied to other split aptamer-based colorimetric sensing system.

Acknowledgments

The authors gratefully acknowledge the Joint Ph.D. Scheme of the University of Science & Technology of China and City University of Hong Kong, the National Natural Science Foundation of China (Nos. 51073146, 21074122, 51103143, 51173175), and Fundamental Research Funds for the Central Universities (No. WK2060200005, 2010).

References

[1] R. Elghanian, J.J. Storhoff, R.C. Mucic, R.L. Letsinger, C.A. Mirkin, Science 277 (1997) 1078–1081.
[2] J.W. Liu, Y. Lu, J. Am. Chem. Soc. 126 (2004) 12298–12305.
[3] J.K. Lim, S.-W. Joo, Appl. Spectrosc. 60 (2006) 847–852.
[4] J.S. Lee, M.S. Han, C.A. Mirkin, Angew. Chem., Int. Ed., 46, 4093–4096.
[5] A.P. Alivisatos, K.P. Johnsson, X. Peng, T.E. Wilson, C.J. Loweth, M.P. Bruchez, P.G. Schultz, Nature 382 (1996) 609–611.
[6] C.A. Mirkin, R.L. Letsinger, R.C. Mucic, J.J. Storhoff, Nature 382 (1996) 607–609.
[7] M. Zheng, A. Jagota, M.S. Strano, A.P. Santos, P. Barone, S.G. Chou, B.A. Diner, M. S. Dresselhaus, R.S. Mclean, G.B. Onoa, G.G. Samsonidze, E.D. Semke, M. Usrey, D.J. Walls, Science 302 (2003) 1545–1548.
[8] D. Nykypanchuk, M.M. Maye, D. van der Lelie, O. Gang, Nature 451 (2008) 549–552.
[9] D.A. Giljohann, D.S. Seferos, W.L. Daniel, M.D. Massich, P.C. Patel, C.A. Mirkin, Angew. Chem., Int. Ed. 49 (2010) 3280–3294.
[10] K. Saha, S.S. Agasti, C. Kim, X. Li, V.M. Rotello, Chem. Rev. 112 (2012) 2739–2779.
[11] R.R. Breaker, Curr. Opin. Chem. Biol. 1 (1997) 26–31.
[12] C. Tuerk, L. Gold, Science 249 (1990) 505–510.
[13] A.D. Ellington, J.W. Szostak, Nature 346 (1990) 818–822.
[14] S.D. Jayasena, Clin. Chem. 45 (1999) 1628–1650.
[15] P. Wang, Y. Song, Y. Zhao, A. Fan, Talanta 103 (2013) 392–397.
[16] C. Xiong, L. Ling, Talanta 89 (2012) 317–321.
[17] J. Liu, Y. Lu, Angew. Chem., Int. Ed. 45 (2006) 90–94.
[18] J. Liu, Y. Lu, Adv. Mater. 18 (2006) 1667–1671.
[19] F. Li, J. Zhang, X. Cao, L. Wang, D. Li, S. Song, B. Ye, C. Fan, Analyst 134 (2009) 1355–1360.
[20] X.L. Zuo, Y. Xiao, K.W. Plaxco, J. Am. Chem. Soc. 131 (2009) 6944–6945.
[21] N. Lu, C. Shao, Z. Deng, Chem. Commun. 0 (2008) 6161–6163.
[22] J. Zhang, L. Wang, D. Pan, S. Song, F.Y.C. Boey, H. Zhang, C. Fan, Small 4 (2008) 1196–1200.
[23] D.-M. Kong, N. Wang, X.-X. Guo, H.-X. Shen, Analyst 135 (2010) 545–549.
[24] X. Xu, J. Zhang, F. Yang, X. Yang, Chem. Commun. 47 (2011) 9435–9437.
[25] N. Dave, J. Liu, Chem. Commun. 48 (2012) 3718–3720.
[26] C. Wu, L. Yan, C. Wang, H. Lin, C. Wang, X. Chen, C.J. Yang, Biosens. Bioelectron. 25 (2010) 2232–2237.
[27] J. Chen, J. Zhang, J. Li, H.-H. Yang, F. Fu, G. Chen, Biosens. Bioelectron. 25 (2010) 996–1000.
[28] L. Kashefi-Kheyrabadi, M.A. Mehrgardi, Biosens. Bioelectron. 37 (2012) 94–98.
[29] Y. Du, S. Guo, H. Qin, S. Dong, E. Wang, Chem. Commun. 48 (2012) 799–801.
[30] J. Chen, L. Zeng, Biosens. Bioelectron. 42 (2013) 93–99.
[31] Q. Wang, J. Huang, X. Yang, K. Wang, L. He, X. Li, C. Xue, Sensor. Actuat. B: Chem. 156 (2011) 893–898.
[32] X. Yang, J. Huang, Q. Wang, K. Wang, L. Yang, X. Huo, Anal. Methods 3 (2011) 59–61.
[33] M.I. Shukoor, M.O. Altman, D. Han, A.T. Bayrac, I. Ocsoy, Z. Zhu, W. Tan, ACS Appl. Mater. Inter. 4 (2012) 3007–3011.
[34] J.J. Zhu, J.J. Zhou, H.P. Huang, J. Xuan, J.R. Zhang, Biosens. Bioelectron. 26 (2010) 834–840.
[35] M. Li, J. Zhang, S. Suri, L.J. Sooter, D. Ma, N. Wu, Anal. Chem. 84 (2012) 2837–2842.
[36] D. Li, A. Wieckowska, I. Willner, Angew. Chem., Int. Ed. 47 (2008) 3927–3931.
[37] J. Liu, Y. Lu, Nat. Protoc. 1 (2006) 246–252.
[38] R.C. Jin, G.S. Wu, Z. Li, C.A. Mirkin, G.C. Schatz, J. Am. Chem. Soc. 125 (2003) 1643–1654.
[39] B. Liu, Y. Cui, D. Tang, H. Yang, G. Chen, Chem. Commun. 48 (2012) 2624–2626.
[40] D.E. Huizenga, J.W. Szostak, Biochemistry 34 (1995) 656–665.
[41] W. Zhao, W. Chiuman, J.C.F. Lam, S.A. McManus, W. Chen, Y. Cui, R. Pelton, M.A. Brook, Y. Li, J. Am. Chem. Soc. 130 (2008) 3610–3618.